Robust Estimation of Pigment Distributions from Multiband Skin Images and Its Application to Realistic Skin Image Synthesis

Motonori Doi[1], Masahiro Konishi[1], Akira Kimachi[1], Shogo Nishi[1], and Shoji Tominaga[2]

[1] Osaka Electro-Communication University, Osaka, Japan
[2] Chiba University, Chiba, Japan

Abstract. This paper describes a robust method for estimating pigment distributions on a skin surface from multiband images. The spatial distributions of the pigments such as melanin, oxy-hemoglobin and deoxy-hemoglobin give rise to a color texture. The distributions are estimated by using the Kubelka-Munk theory. The accuracy of estimating the pigment distributions is affected by a fine texture of sulcus cutis and a broad texture of shade caused by three-dimensional body shape. In order to separate these textures from the color texture, wavelet-based multi-resolution analysis (MRA) is applied to the multiband images before the pigment estimation, because the textures of sulcus cutis and shade predominantly have low and high spatial frequency components in the multiband skin images, respectively. Realistic skin image is synthesized from modified pigment distributions with additional features such as stain, inflammation and bruise by changing the concentrations of melanin, oxy-hemoglobin and deoxy-hemoglobin, respectively. The experimental results of skin image synthesis show good feasibility of the proposed method.

Keywords: Skin, Pigment distribution estimation, Multiband image, The Kubelka-Munk theory, Multi-resolution analysis, Skin image synthesis.

1 Introduction

Various texture patterns appear on the surface of human skin. For example, we perceive moles, veins, inflammation and bruise as skin surface textures of dark brown spots, bluish streaks, and red and purple marks, respectively. These color features are caused by high concentration of pigments in the skin. Specifically, melanin, oxy-hemoglobin, and deoxy-hemoglobin make the skin look brownish, reddish, and purplish, respectively. The skin surface also has a fine texture caused by minute grooves called sulcus cutis, and a broad texture of shade caused by three-dimensional body shape. These textures are superimposed on the pigment derived texture.

A. Fusiello et al. (Eds.): ECCV 2012 Ws/Demos, Part II, LNCS 7584, pp. 421–430, 2012.

The analysis and synthesis of these texture features on human skin are important in several research areas, such as computer graphics, medical imaging and cosmetics development. Especially, in computer graphics, the detailed description of human skin is essential for realistic image rendering. It is difficult to generate photorealistic skin image, because the skin surface includes various textures. When we put a conspicuous pattern on a skin image, it is difficult to match its skin color and texture to the color and texture of the surrounding area. Therefore the skin image rendering includes precise color reproduction and synthesis of the complicated tissue patterns. For the realistic skin image rendering, the decomposition of real skin image into texture components and the reconstruction of modified texture components into skin image are required. Our previous work[1] decomposed RGB color image of skin into texture components. Then, images with enhanced texture components were synthesized. However, the method cannot control each texture with different pigment distribution. Tsumura et al. proposed a method for skin texture analysis and synthesis of facial images based on independent component analysis[2]. Their work considered neither the deoxy-hemoglobin absorption nor the texture of sulcus cutis on the skin surface. The skin color image analysis requires accurate estimation of the pigment distributions from real images. It is difficult, however, to distinguish the concentration of oxy-hemoglobin and deoxy-hemoglobin in the RGB color space. Moreover, the superimposed textures of sulcus cutis and shade introduce additional spatial variation in a skin image, hindering accurate estimation of the pigment distributions.

To solve these problems, the present paper proposes a method for robustly estimating the pigment distributions on a human skin surface from multiband images, and synthesizing realistic skin color images using the estimation results. We apply the estimation method of spectral reflectance of skin surface based on the Kubelka-Munk theory[3] to estimate the pigment distributions from multiband images. This method can estimate the concentrations of oxy-hemoglobin and deoxy-hemoglobin, as well as melanin, separately by taking account of the spectral absorption of these pigments. To improve the estimation accuracy, multiresolution analysis (MRA) is adopted to the multiband images as a pre-image processing. The MRA effectively separates the textures of sulcus cutis and shade from the color texture associated with the pigment distributions. At the image synthesis stage, artificial images of human skin with additional features such as stain, inflammation and bruise are realistically produced in combination with the separated textures of sulcus cutis and shade, by changing the estimated distributions of melanin, oxy-hemoglobin and deoxy-hemoglobin.

2 Features of Skin Surface

Skin surface consists of layers of turbid medium. Fig.1(a) shows the rough sketch of skin surface. Top layer of horny substance is almost transparent and has fine grooves of skin surface. Fig.1(b) shows the texture of fine grooves by sulcus cutis. Skin surface roughness by sulcus cutis gives fine texture to skin. Epidermis

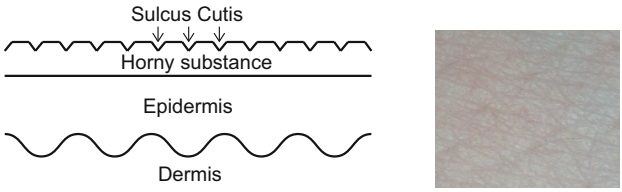

(a) Rough sketch of skin layers (b) Sulcus cutis

Fig. 1. Skin layers and sulcus cutis

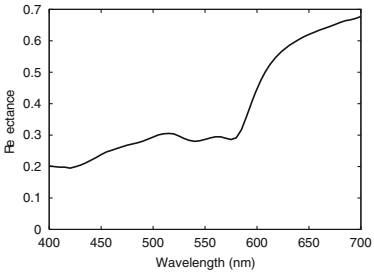

Fig. 2. Spectral reflectance of skin

includes pigments of melanin, and dermis includes oxy-hemoglobin and deoxy-hemoglobin. The spatial color distribution on skin surface is determined by these pigment concentrations. Shade appears on the skin surface of curved body shape.

Surface reflectances of natural objects including human skin are spectrally high-dimensional[4]. However, the conventional three-channel color cameras often cannot capture small color differences on object surfaces. The analysis of concentration of each pigment requires precise color information. In such a case, a multiband imaging system with more than three different spectral bands is useful to detect the difference in pigmentation.

The spectral reflectance of skin is influenced by the interaction of pigments inside the skin tissue. Fig.2 shows spectral reflectance curves of skin. A basic feature of the reflectance curves is that the reflectance increases almost monotonically as the wavelength increases. A special feature is the "W" shaped or "U" shaped hollow in the range from 500nm to 600nm. This change in reflectance is caused by the absorption of oxy-hemoglobin. Thus, the narrow band imaging is required to capture the hollow of skin reflectance curve.

3 Estimation of Pigment Distributions from Multiband Skin Images

We propose a multispectral analysis method of pigment distributions on skin surface. Fig.3 shows the scheme of pigment distribution estimation. First of all,

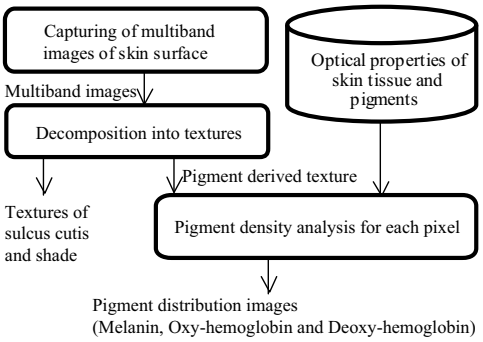

Fig. 3. Scheme of pigment distribution estimation

the multiband images of skin are captured. The captured images are decomposed into texture components by the MRA. The shade texture and sulcus cutis texture are separated from multiband images for accurate pigment density estimation. Then, pigment density for each pixel is estimated. As the result of the estimation, pigment distribution images are obtained.

3.1 Capturing Multiband Images

In the multiband imaging of skin, we select suitable spectral bands to capture the absorbance of pigments. The present multiband imaging system is composed of a monochrome camera and a programmable light source (Gooch&Housego, OL490), which can emit light with arbitrary spectral-power distribution. The programmable light source is useful for the band selection. The spectral reflectance of skin shows the W shaped or U shaped hollow by the absorption of hemoglobin in the range from 500nm to 600nm. Therefore, the spectral image in this range is captured with narrow band width of 10nm. In the other range, the band width is set to 30nm. In all, 17 band images are captured. The exposure time for each band is controlled for sufficient contrast. The output of the camera is normalized by a standard white.

3.2 Decomposing Images into Textures

The MRA with wavelet functions[5] is applied for the decomposition of images. The MRA is done as follows. First, an image is decomposed into four components as shown in Fig.4(a). These are components of low frequency for column and row (LL), low frequency for column and high frequency for row (LH), high frequency for column and low frequency for row (HL), and high frequency for column and row (HH). This is the decomposition at level depth -1. Then, the LL component for column and row is decomposed into four components again as shown in Fig.4(b). This is the decomposition at level depth -2. By repetition of the decomposition, the levels are from 0 for the original image to -m for the

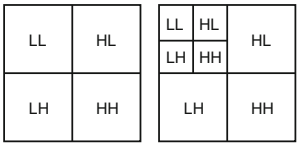

(a) Level -1 (b) Level -2

Fig. 4. Multi-resolution analysis

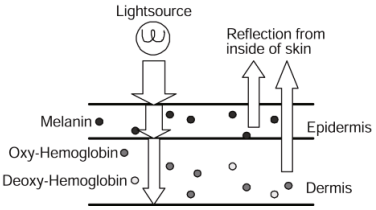

Fig. 5. Skin optics model

DC component in the case of a square image with 2m-by-2m pixels. This image analysis is useful for the separation of some texture patterns.

Sulcus cutis texture is included in high frequency levels. The shade caused by body shape appears in low frequency levels. We detect the shade from low frequency levels of the image taken under long wavelength illumination. The skin image doesn't contain clear pigment absorbance and fine grooves under long wavelength illumination. Then, the shade and sulcus cutis pattern are separated from multiband images.

3.3 Skin Reflectance Analysis Based on the Kubelka-Munk Theory

The relationship between spectral reflectance of skin and pigment concentrations is studied using the Kubelka-Munk theory[6,7]. It is known that the Kubelka-Munk theory is available for calculating the optical values of reflectance and transmittance within a layer consisting of turbid materials. A method based on the Kubelka-Munk theory was presented to estimate the density parameters of pigments and the skin surface reflectance[3].

The skin optics model for the skin spectral reflectance is assumed. The skin model is the two turbid layers of the epidermis including melanin and dermis including hemoglobin as shown in Fig.5. Horny substance that doesn't contain pigments is not considered in this model. The incident light penetrating the skin surface is absorbed and scattered in these two layers. The body reflectance function of the skin surface $R_b(\lambda)$ is described as a function of wavelength as

$$\begin{aligned} R_b(\lambda) &= R_e(\lambda) + \frac{T_e^2(\lambda) R_{dt}(\lambda)}{1 - R_e(\lambda) R_{dt}(\lambda)} \\ R_{dt}(\lambda) &= R_d(\lambda) + \frac{T_d^2(\lambda)}{1 - R_d(\lambda)} \end{aligned} \tag{1}$$

where $R_e(\lambda)$ and $T_e(\lambda)$ are, respectively, the spectral reflectance and transmittance of the epidermis, $R_d(\lambda)$ and $T_d(\lambda)$ are the spectral reflectance and transmittance of the dermis, respectively. The reflectance of tissues under dermis is regarded as 1.

The spectral reflectances and transmittances of the respective layers are given as follows:

Epidermis:

$$\begin{aligned} R_e(\lambda) &= \frac{1}{a_e(\lambda)+b_e(\lambda)\coth b_e(\lambda)S_e(\lambda)D_e} \\ T_e(\lambda) &= \frac{b_e(\lambda)}{a_e(\lambda)\sinh b_e(\lambda)S_e(\lambda)D_e+b_e(\lambda)\cosh b_e(\lambda)S_e(\lambda)D_e} \\ a_e(\lambda) &= \frac{S_e(\lambda)+K_e(\lambda)}{S_e(\lambda)}, b_e(\lambda) = \sqrt{a_e^2(\lambda)-1} \end{aligned} \tag{2}$$

Dermis:

$$\begin{aligned} R_d(\lambda) &= \frac{1}{a_d(\lambda)+b_d(\lambda)\coth b_d(\lambda)S_d(\lambda)D_d} \\ T_d(\lambda) &= \frac{b_d(\lambda)}{a_d(\lambda)\sinh b_d(\lambda)S_d(\lambda)D_d+b_d(\lambda)\cosh b_d(\lambda)S_d(\lambda)D_d} \\ a_d(\lambda) &= \frac{S_d(\lambda)+K_d(\lambda)}{S_d(\lambda)}, b_d(\lambda) = \sqrt{a_d^2(\lambda)-1} \end{aligned} \tag{3}$$

where $S_e(\lambda)$ and $S_d(\lambda)$ are spectral scattering coefficients in epidermis and dermis, respectively. The spectral absorption coefficients $K_e(\lambda)$ and $K_d(\lambda)$ in the two layers are determined by the pigments in the following forms:

$$\begin{aligned} K_e(\lambda) &= w_m K_m(\lambda) \\ K_d(\lambda) &= w_h K_h(\lambda) + w_{dh} K_{dh}(\lambda) \end{aligned} \tag{4}$$

where $K_m(\lambda)$, $K_h(\lambda)$, and $K_{dh}(\lambda)$ represent the spectral-absorption coefficients of melanin, oxy-hemoglobin, and deoxy-hemoglobin, respectively. The constant coefficients w_m, w_h, and w_{dh} represent the weights of the pigment absorption coefficients.

For applying the estimation algorithm to real measurements, we need the optical and histological data of skin tissue. The spectral absorption data, the spectral scattering data, and the layer thickness values published in Refs[8,9] are used in this paper.

4 Skin Image Synthesis

Realistic skin image is synthesized from modified pigment distributions. Fig.6 shows the scheme of skin image synthesis.

First, the pigment density at a certain area in the pigment distribution image is modified by image editing software. Then, the multispectral pigment derived texture is generated from the modified pigment distribution image by the method based on the Kubelka-Munk theory. Next, the multispectral pigment derived texture, the sulcus cutis texture and shade texture are composed into multiband

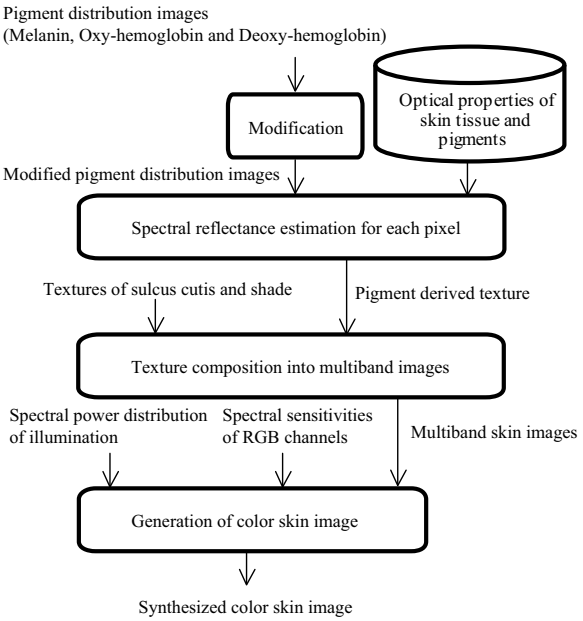

Fig. 6. Scheme of skin image synthesis

skin images by the MRA. Finally, an RGB color image of skin is produced from a set of multiband skin images. We should note that color appearance of the skin image depends on the RGB spectral-sensitivity functions of the camera used.

5 Experiments

5.1 Spectral Image of Skin

We captured multiband images of skin surface on inner forearm (Male, 41 years old). A square area of 2cm × 2cm was extracted from the multiband image as an image of 256 × 256 pixels. Fig.7 shows an image sequence of 17 bands and the RGB image. The extracted area included mole and vein.

5.2 Analysis Results of Skin Image

The MRA was applied to all band images. We used the Daubechies wavelet with wavelet order equal to 10 for the MRA. The wavelet order was determined empirically. Images were decomposed into 8-level texture component. We determined three high frequency levels (Level 1, 2, 3) as sulcus cutis texture. The shade caused by body shape was extracted from Level 7 and 8 of the image taken under long wavelength illumination. Then, the shade and sulcus cutis patterns

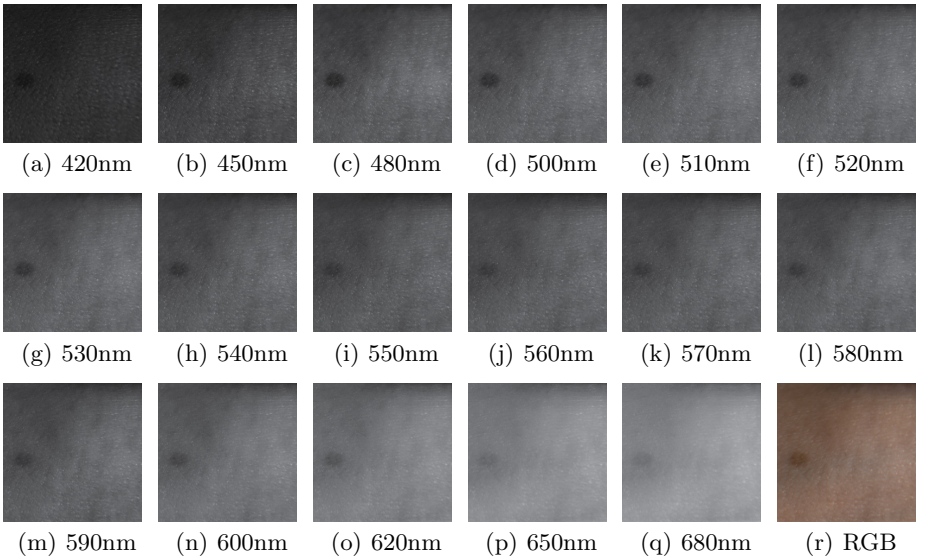

Fig. 7. Image sequence of 17 bands and the RGB image including mole and vein

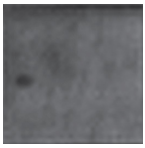

Fig. 8. Band image without shade and sulcus cutis texture patterns(550nm)

were separated from multiband image. Fig.8 shows an example of spectral image without shade and sulcus cutis patterns. Then, the pigment density analysis based on the Kubelka-Munk theory was done for multiband images.

The pigment distribution images are shown in Fig. 9. In these images, bright pixels shows high pigment density and dark pixels shows low pigment density. Mole showed the high concentration of melanin. Vein appeared in deoxy-hemoglobin distribution image. The distributions of oxy-hemoglobin and deoxy-hemoglobin are detected independently.

5.3 Synthesis Results of Skin Image

In the synthesis, we generated three types of images; 1) addition of melanin spot (stain), 2) addition of oxy-hemoglobin spot (inflammation), 3) addition of deoxy-hemoglobin spot (bruise). Fig.10 shows the modified pigment distribution image with the high concentration spot of each pigment. Fig.11 shows the synthesized skin color images. The CIE D65 was supposed as the illumination in

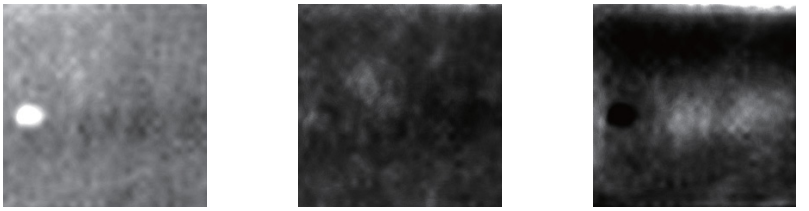

(a) Melanin (b) Oxy-hemoglobin (c) Deoxy-hemoglobin

Fig. 9. Pigment distribution images. (Bright pixels show high pigment density.)

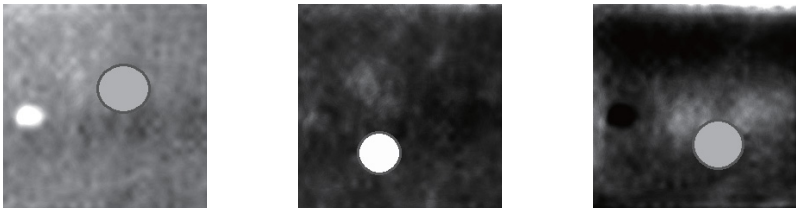

(a) Melanin (b) Oxy-hemoglobin (c) Deoxy-hemoglobin

Fig. 10. Modified pigment distribution images with pigment concentration area

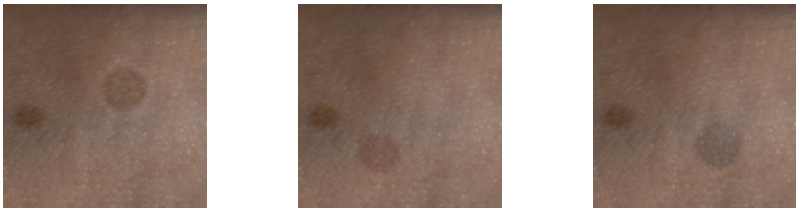

(a) Melanin (b) Oxy-hemoglobin (c) Deoxy-hemoglobin

Fig. 11. Results of texture synthesis for the addition of pigment concentration area

the synthesis. The colors of added spots are realistic, and the textures of the spots are matched to the textures of the surrounding area. These images show the feasibility of the proposed method.

6 Conclusions

This paper proposed a method for the estimation of pigment distributions from multiband skin images, and synthesizing realistic skin images including high concentrations of pigments. By using multiband images, pigment distribution of melanin, oxy-hemoglobin and deoxy-hemoglobin are estimated by the method based on the Kubelka-Munk theory. For accurate estimation, textures of shade

and sulcus cutis are separated from multiband images by the MRA in advance of the estimation. Realistic skin image is synthesized from modified pigment distributions by changing the estimated distributions of melanin, oxy-hemoglobin and deoxy-hemoglobin. Experimental results showed that synthesized skin images for the addition of pigment concentrations of stain, inflammation and bruise were realistic. The results showed good feasibility of the proposed method.

Acknowledgments. This work was supported by Grants-in-Aid for Scientific Research (KAKENHI) (No. 23135529).

References

1. Doi, M., et al.: Image Analysis and Synthesis of Skin Color Textures by Wavelet Transform. In: Proceedings of IEEE Southwest Symposium on Image Analysis and Interpretation 2006, pp. 193–197 (2006)
2. Tsumura, N., et al.: Image-based skin color and texture analysis/synthesis by extracting hemoglobin and melanin information in the skin. In: Proceedings of SIGGRAPH 2003, pp. 770–779 (2003)
3. Doi, M., et al.: Spectral Reflectance Estimation of Human Skin and Its Application to Image Rendering. Journal of Image Science and Technology 49, 574–582 (2005)
4. Tominaga, S.: Spectral imaging by a multi-channel camera. Journal of Electronic Imaging 8, 332–341 (1999)
5. Mallat, S.G.: A theory for multiresolution signal decomposition: the wavelet representation. IEEE Transactions on Pattern Analysis and Machine Intelligence 11, 674–693 (1989)
6. Kubelka, P.: New Contributions to the Optics of Intensely Light-Scattering Materials. Part I. Journal of the Optical Society of America 38, 448–457 (1948)
7. Kubelka, P.: New Contributions to the Optics of Intensely Light-Scattering Materials. Part II. Journal of the Optical Society of America 44, 330–335 (1954)
8. Anderson, R.R., Parrish, J.A.: The Optics of Human Skin. Journal of Investigative Dermatology 77, 13–19 (1981)
9. Van Gemert, M.J.C., et al.: Skin Optics. IEEE Transactions on Biomedical Engineering 36, 1146–1154 (1989)